CHEMICAL ENGINEERING TRANSACTIONS
VOL.

A publication of AIDIC
The Italian Association of Chemical Engineering
Online at www.cetjournal.it

Guest Editors:

ISBN 978-88-95608-xx-x **ISSN** 2283-9216

The Set up of an experimental testing rig to measure time and space temperature profiles in Laser Sintering of Polymeric powders

Balaji Soundararajan[a]*, Daniele Sofia[a, b], Diego Barletta[a] and Massimo Poletto[a]

[a] Dipartimento di Ingegneria Industriale - Università di Salerno, *Via Giovanni Paolo II, 132 – 84084 Fisciano (SA) –Italy*
[b]Sense Square Srl, *Piazza Vittorio Emanuele 10, Penta 84084 , Salerno, Italy*
bsoundararajan@unisa.it

Selective Laser Sintering (SLS) is the most common type of Additive Manufacturing (AM) process using granular materials which has the potential to revolutionize the manufacturing industry. However, in the layer-wise build-up of the three-dimensional specimen, the complex laser-material interactions and the poor selection of associated process parameters can give rise to an increase to a number of defects of the artifacts. In fact, the temperature distribution along the surface and in depth at the laser spot, which are strongly affected by the thermal conductivity of the powder bed, do affect the hatch distance and the thickness of the powder layer, as well as on the quality of the final artifact. In this study, a laser sintering experimental set-up, equipped with an Infra-red thermographic camera and a K-type thermocouple, is built to measure the temperature distribution at the surface and 1mm below the surface in a special Polyamide 12 (PA12) powder bed. A one-watt stationary diode laser is used as heat source on samples characterized by various particle size distributions (PSD). Using the set-up, an accurate in-situ thermal characterization of the powder bed along with heat distribution study can be performed. Preliminary tests were conducted and the pixelwise temperature profile along the surface and temperature at the depth of 1mm below the surface of the powder bed has been reported. On the basis of the results, it is possible to provide good estimates of the global energy balances on the system, which are essential in evaluating the energy required to optimize the sintering and melting process of the polymeric powders.

1. Introduction

In the manufacturing industry, usage of granular materials in Additive Manufacturing (AM) of products using Laser based powder bed fusion (L-PBF) technique has garnered special interest all over the world due to its ability to manufacture very complex parts at relatively lower costs compared to conventional techniques. The parts are built by sintering or melting powders added layer by layer and the design freedom and part optimization strategies offered by this process are ideal for industries such as aerospace, automotive and medical where manufacturing volumes are usually low and costs are high (Pereira et al., 2019). Despite continuous technological advancements in the field of AM, inability to repeat the process at required quality level acts as a hindrance for industrial breakthrough (Grasso & Colosimo, 2017). SLS is a complex phenomenon which involves laser-material interactions and heat generated is dissipated through heat conduction in powder bed, convection and radiation (Sofia et al., 2015). In polymeric powders where the temperatures involved are much lower than metals and ceramics, conduction is the major means of heat dissipation and radiation is usually neglected (Kolossov et al., 2004). Generally, an Infra-red (IR) thermography based process monitoring is used to measure the layer temperature, melt pool formations and powder bed homogeneity during the SLS process (Alldredge et al., 2018; Dinwiddie et al., 2016). A deeper understanding of process parameters that influences the thermo-mechanical behaviour of the final specimen is required. One such parameter is the layer thickness of the specimen, which is influenced by the depth of penetration of laser beam in the powder bed and associated heat distribution along the depth and surface. Layer thickness determines the geometric accuracy of the final part and also the manufacturing time required (Kozak & Zakrzewski, 2018). Layer thickness also influences the powder bed preparation and compaction during the SLS process which in turn determines the mechanical

strength of the part (Sofia et al., 2019). Lupo et al., (2019) emphasised the need for calibration of numerical models such as Finite Element Modelling (FEM) or Discrete Element Modelling (DEM) in the SLS domain using experimental techniques. Thermal conductivity of the powder bed is a temperature-dependent material property and is defined as the rate at which heat is conducted through the body and usually measured as Watt per meter Kelvin (W/mK). Thermal conductivity of powders are significantly different and lower than that of the particle material as the contact area in powder bed is smaller. Generally, authors use 'effective thermal conductivity' which is determined numerically (Moser et al., 2016; Tsory et al., 2013) or through transient plane source (TPS) experimental technique (Yuan et al., 2013). However, an environment more closer to actual SLS machine would help in determining the real time thermal conductivity and the heat flow into the powder bed, thereby identifying the optimum layer thickness required. This paper describes about a new experimental setup built to achieve such objective and a special carbon black Polyamide 12 (PA12) powder is used for this purpose. Carbon black treated PA12 offers higher energy absorption and faster heating than normal PA12 which helps in testing the system at a reduced laser power. An Infra-red (IR) thermography based camera is positioned at the top and a provision in the powder bed is provided to insert a K-type thermocouple to measure the temperatures both at the surface and 1mm below the powder bed.

2. Apparatus and procedure

The Computer Aided Design (CAD) model and the actual experimental setup are shown in Figure 1. A stationary one-watt diode Laser (LDM-405-1000 type) which operates in the wavelength between 400 to 410 nm is used as the heat source and is attached to an aluminum profile right above the powder bed. The Laser beam has a diameter of 100 microns. A thermal camera (Seek compact, USA) is positioned at back of the setup overlooking the powder bed at 45° angle from the horizontal. The thermal camera is mounted on a 'Raspberry pi' computer board, which in turn is mounted on an aluminum profile. The communication to control the thermal camera is managed in a Virtual Network Computing (VNC) environment using Wi-Fi for connection.

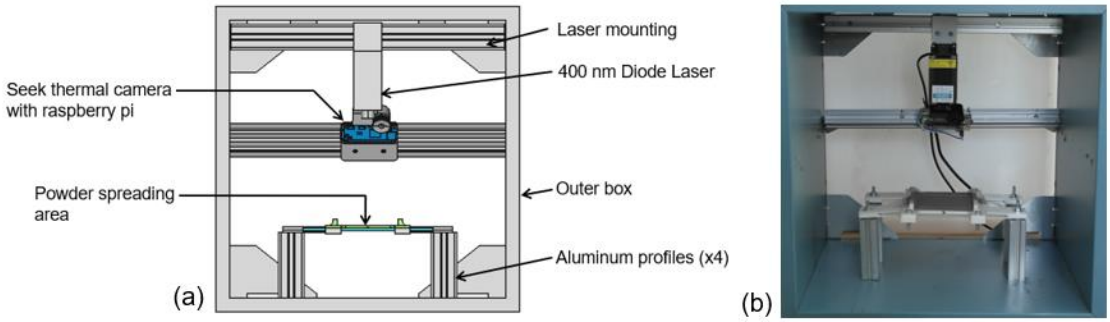

Figure 1: (a) CAD model of the experimental assembly and (b) actual setup

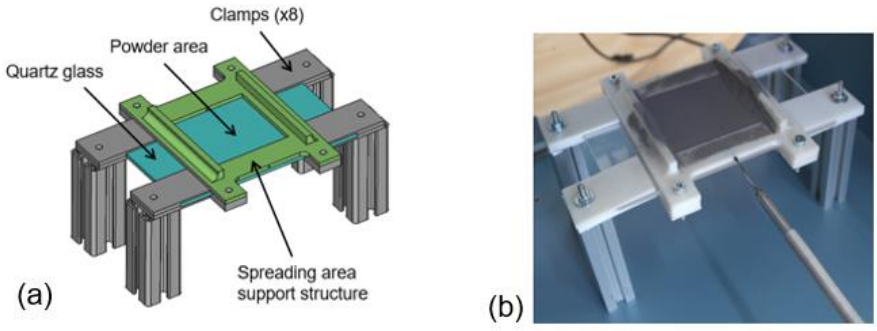

Figure 2: (a) CAD model of lower powder spreading assembly and (b) actual setup with the K-type thermocouple inserted in the powder bed.

The Seek thermal camera has a resolution of 206 x 156 pixels with a Field of View (FOV) of 36°. It measures in long range IR between 7.5 to 14 microns and has a frame rate up to 9Hz. The sensor pixel pitch is 12 µm. The

characteristics of the camera are presented in *Table 1*. A high accuracy programmable digital temperature sensor Bosch MCP9808 with a temperature accuracy of ±0.25°C is used to measure the internal build chamber temperature which is used as a reference in calibrating the data from thermal camera.

Table 1: Characteristics of thermal camera

Thermal Camera	Pixels	Field of view	Maximum temperature	Sensor type	Spectral range	Frame rate
SEEK compact	206 x 156	36°	330°C	Vanadium oxide	7.5-14µm	<9Hz

The bottom assembly provides the powder bed area supported by a Quartz glass mounted using clamps. The Quartz glass is 3mm thick and has a dimension of 150mmx100mm. A frame, the support structure, held by the clamps, defines the margins of the powder bed area on the Quartz glass. The resulting powder bed fills 60x60x3.2mm volume. The clamps and the support structure are made of Poly-Lactic Acid (PLA) material. They were purposely designed and built by using Fused Deposition Modelling method of AM. The entire setup stands on four aluminium profiles. Doors are used to cover the set-up during experimentation. The powder bed spreading is carried out on top of the Quartz glass and is guided by the bed support structure. The powder bed surface is exposed to laser heating. A K-type thermocouple is inserted into the powder bed 1mm below the surface as shown below in . The K-type thermocouple (chromel-alumel) is a most common type of thermocouple used in temperature measurements which uses thermoelectric effect to measure. Experiments were conducted in a chamber environment which is at atmospheric pressure and room temperature.

The powder used in these experiments are specially treated carbon black PA12 powder which is an industrial grade polymer (Nylon) and has a density of 950 Kg/m^3, melting temperature of 180°C and heat deflection temperature of 177°C.

Tests were conducted by firstly inserting the K-type thermocouple into the powder bed area followed by preparation of powder bed with PA12 powder using a spreading tool. Laser heating of the powder bed was done till the melting temperatures were reached. The thermal camera uses uncooled vanadium dioxide based microbolometer which is a type of infrared detector. The detector is sensitive to infrared energy and once the element increases in temperature, the element resistance changes and, measured, is the variable that is processed to obtain the local temperature values. Pixel-wise raw data measured by thermal camera is converted into useful temperature information using a calibrated equation derived from the experiments as shown below,

$$\text{Surface Temperature, T} = (0.0457X) - 687.26 \quad (1)$$

Where *X* is the raw pixel value transmitted from the thermal camera. The Instantaneous Field of View (IFOV) is the angular projection cone of one of the detector's pixels in the IR image and is usually measured in milliradians (mRad). The area each pixel can see depends upon the distance from the target for a given field of view of the camera. In order to calculate IFOV from the entire Field of View (FOV) expressed in degrees (36°), equation 2 and 3 are used (Pušnik & Geršak, 2021). The IFOV is first calculated in mRad which is then converted into mm using equation 3. The powder bed heat affected zone is 100mm away from the sensor.

$$IFOV\ (mRad) = \left[\frac{FOV}{No.of\ pixels}\right] X\ \left[\frac{\pi}{180} X1000\right] \quad (2)$$

$$IFOV\ (mm) = \left[\frac{IFOV\ (mRad)}{1000} X100\right] \quad (3)$$

The IFOV calculations reveal that the distances corresponding to position measured for consecutive pixels in the thermal image is 0.31mm. Simultaneously, measurements from thermocouple are recorded as well.

3. Results and discussions

The powder bed surface temperatures in the vicinity of the melt pool is shown below in Figure 3. The temperature close to the melting point of the special carbon black PA12 powder is recorded to be 179.17°C and is achieved after 64.5 sec of the laser switched on. A nearly symmetric temperature profile has been witnessed. The wider temperature distribution is due to the fact that powders with carbon black increases the thermal conductivity of

the powder. Error bars in figure 3 are the standard deviation expected for the temperature measurement, though profile variability due to uncontrolled variables such as the ambient temperature need to be better investigated in the future, with repeated experiments.

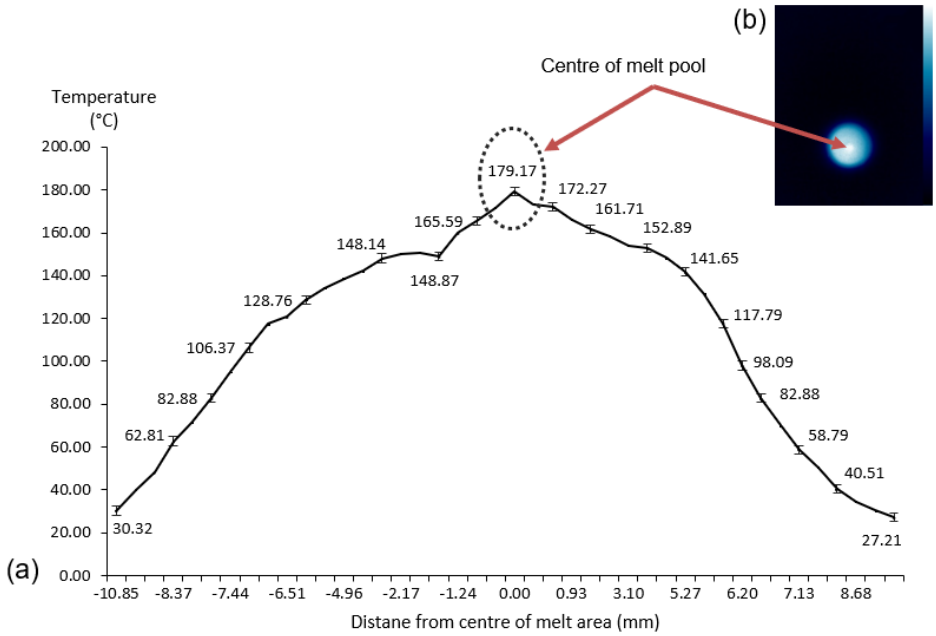

Figure 3: (a) Temperature profile in the vicinity of the heat affected zone with an error bar of 2°C. The maximum temperature reached at 64.5 sec is 179.17°C which is close to the melting temperature of PA12 powder (b) Actual thermal image

(a)

148.18	146.22	148.41	147.40	149.92	147.18	152.34	154.03	152.43	151.15	149.32
146.13	144.62	152.52	151.52	151.65	158.19	156.41	153.53	154.95	152.48	150.83
151.29	148.27	147.77	159.74	154.44	162.44	162.99	162.90	157.09	152.57	155.77
149.83	151.20	162.30	163.67	168.47	168.70	167.15	170.16	160.20	156.64	155.54
152.11	153.07	158.28	159.56	171.95	170.35	169.48	170.99	164.41	162.03	157.32
148.87	159.79	162.71	165.59	171.53	179.17	173.27	172.27	166.32	161.71	158.33
148.36	153.62	167.24	164.86	171.72	174.55	172.31	168.75	166.96	162.49	158.78
143.52	153.30	166.96	156.45	168.66	172.81	165.14	170.21	166.74	157.05	161.57
144.85	148.46	152.80	163.54	170.21	162.90	170.57	166.60	165.41	162.94	158.65
146.40	149.60	151.65	160.34	163.58	163.77	166.37	165.59	162.49	157.00	156.04
150.15	141.60	150.24	143.61	157.73	158.56	157.14	161.39	162.07	152.16	159.97

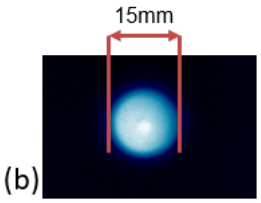

Figure 4: (a) Sample heat affected zone pixel-wise temperature matrix derived from thermal camera raw data. Peak temperature of 179.17°C is marked (b) actual thermal image

A pixel-wise temperature data matrix of the heat affected zone generated from the raw data of thermal camera is presented above in *Figure **4**: (a) Sample heat affected zone pixel-wise temperature matrix derived from thermal camera raw data. Peak temperature of 179.17°C is marked (b) actual thermal imageFigure **4***. The size of the heat affected zone is measured to be 15 mm. The data is available for the entire thermal image. Similarly, *Figure **5*** shows the temperature profile 1mm right below the laser impacted surface. The peak temperature reached is 103.3°C at 64.5 sec. This shows that the layer thickness can still be reduced to less than 1mm in order to achieve sintering temperatures for the given PA12 powder and input laser power. The cool down phase is faster as compared to heating and is attributed to both heat conduction and convection. The powder bed is homogenous due to uniform spreading of the powder and the inhomogeneity in temperature distribution is reduced as the chamber is completely closed and insulated. The limited temperatures reached, and the granular form of the bed ensure that in the proposed experiment no significant residual stress should be found in the cooling phase, affecting the heat exchange.

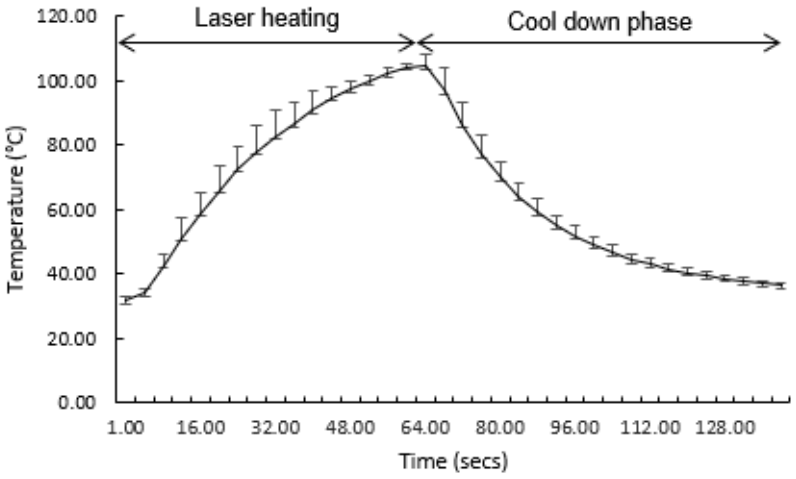

Figure 5: Thermocouple reading 1mm below the powder bed surface with 1σ standard deviation error bar

Due to the slender nature of the K-type thermocouple, it is difficult to accurately measure the temperature right below the laser heating zone. Several tests were conducted by inserting the thermocouple inside the powder bed and measurements with an error bar of 1σ standard deviation is considered.

4. Conclusion

An experimental setup has been built to measure the temperature profile in a powder bed both on the surface and under the surface using IR thermography and thermocouple. Measurements were made 1mm below the surface and the temperatures recorded are much lesser than the sintering temperature of PA12. This shows that the layer thickness can be further minimized for the given material. This experimental setup shall be used to evaluate the energy balance in a SLS system. Temperature profile variability need to be better investigated in the future to highlight the effect of uncontrolled variables such as the ambient temperature.

Acknowledgment

This work has received funding from the European Union's Horizon 2020 research and innovation programme under the Marie Skłodowska-Curie grant agreement MATHEGRAM No 813202.

References

Alldredge, J., Slotwinski, J., Storck, S., Kim, S., Goldberg, A., & Montalbano, T. (2018). In-Situ monitoring and modeling of metal additive manufacturing powder bed fusion. *AIP Conference Proceedings*. https://doi.org/10.1063/1.5031504

Dinwiddie, R. B., Kirka, M. M., Lloyd, P. D., Dehoff, R. R., Lowe, L. E., & Marlow, G. S. (2016). Calibrating IR cameras for in-situ temperature measurement during the electron beam melt processing of Inconel 718 and Ti-Al6-V4. *Thermosense: Thermal Infrared Applications XXXVIII*. https://doi.org/10.1117/12.2229070

Grasso, M., & Colosimo, B. M. (2017). Process defects and in situ monitoring methods in metal powder bed fusion: A review. In *Measurement Science and Technology*. https://doi.org/10.1088/1361-6501/aa5c4f

Kolossov, S., Boillat, E., Glardon, R., Fischer, P., & Locher, M. (2004). 3D FE simulation for temperature evolution in the selective laser sintering process. *International Journal of Machine Tools and Manufacture*. https://doi.org/10.1016/j.ijmachtools.2003.10.019

Kozak, J., & Zakrzewski, T. (2018). Accuracy problems of additive manufacturing using SLS/SLM processes. *AIP Conference Proceedings*, *2017*(October). https://doi.org/10.1063/1.5056273

Moser, D., Pannala, S., & Murthy, J. (2016). Computation of Effective Thermal Conductivity of Powders for Selective Laser Sintering Simulations. *Journal of Heat Transfer*. https://doi.org/10.1115/1.4033351

Pereira, T., Kennedy, J. V., & Potgieter, J. (2019). A comparison of traditional manufacturing vs additive manufacturing, the best method for the job. *Procedia Manufacturing*. https://doi.org/10.1016/j.promfg.2019.02.003

Pušnik, I., & Geršak, G. (2021). Evaluation of the size-of-source effect in thermal imaging cameras. *Sensors (Switzerland)*. https://doi.org/10.3390/s21020607

Sofia, D., Granese, M., Barletta, D., & Poletto, M. (2015). Laser sintering of unimodal distributed glass powders of different size. *Procedia Engineering*. https://doi.org/10.1016/j.proeng.2015.01.180

Sofia, D., Lupo, M., Barletta, D., & Poletto, M. (2019). Validation of an experimental procedure to quantify the effects of powder spreadability on selective laser sintering process. *Chemical Engineering Transactions*. https://doi.org/10.3303/CET1974067

Tsory, T., Ben-Jacob, N., Brosh, T., & Levy, A. (2013). Thermal DEM-CFD modeling and simulation of heat transfer through packed bed. *Powder Technology*. https://doi.org/10.1016/j.powtec.2013.04.013

Yuan, M., Diller, T. T., Bourell, D., & Beaman, J. (2013). Thermal conductivity of polyamide 12 powder for use in laser sintering. *Rapid Prototyping Journal*. https://doi.org/10.1108/RPJ-11-2011-0123